Reconfigurable Identical and Complementary Chirp Dual-LFM Signal Generation Subjected to Dual-Beam Injection in a DFB Laser

Hao Chen, Pei Zhou, Limin Zhang, Snehi Bassi, Bikash Nakarmi, *Member, IEEE, Member, OSA*, and Shilong Pan, *Senior Member, IEEE, Fellow, OSA*

***Abstract*—A photonic approach for identical and complementary chirp dual-linear frequency modulation (LFM) signal generation using an optical injection in a distributed feedback (DFB) laser is proposed and experimentally demonstrated. The proposed scheme is based on the redshift of the emission frequency in the DFB laser, and the nonlinear dynamics in the periodic oscillation of the DFB laser subjected to an optical injection. In the proposed scheme, two optical beams from master lasers, one with varying optical power and another with constant optical power, are injected to the slave laser, a DFB laser. The redshift of the mode in slave laser is due to the injection of the beam with varying optical power, which changes the frequency detuning of the injected beams and the mode of slave laser. Hence, a dual-LFM signal with a large time-bandwidth product (TBWP) is observed. Whether two beams are injected to the slave laser with positive frequency detunings or opposite frequency detunings, dual-LFM signal with the combinations of linearly increasing or/and decreasing frequency is obtained. With the proposed scheme, identical and complementary chirp dual-LFM signals with the same period of 1.3 μs have been obtained. The measured bandwidths for both LFM signals are 7 GHz (LFM1: 16.0-23.0 GHZ; LFM2: 25.0-32.0 GHz) with a TBWP of 9100. The generated dual-LFM signal has flexibility in tuning the center frequency and reconfiguring different IEEE radar bands.**

***Index Terms*—DFB laser, linear frequency modulation signal, optical injection.**

I. Introduction

LINEAR frequency modulation (LFM) signal is one of the most typical microwave waveforms for radar systems to achieve an extensive detection range and a high range resolution [1]. Conventionally, LFM signals are generated using a voltage-controlled microwave oscillator [2], surface acoustic wave filter [3], or a direct digital synthesizer [4] in the electrical domain, which possess the limitation on the flexibility and reconfigurability in the center frequency and the bandwidth, limiting the applications of modern radars for distance measurement, cognition of target, and imaging.

To overcome the bottleneck of LFM signal generation by electrical methods, several photonics techniques with reconfigurable features in terms of improved frequency range and time-bandwidth product (TBWP) have been proposed [5]–[14]. These methods include spectral shaping and frequency-to-time mapping (FTM), which usually contains an optical spectral shaper and a dispersive element [5]–[7]; temporal pulse shaping that utilizes optical dispersive medium and optical interference of pulsed lights [8], [9]; photonic microwave frequency multiplication using optical frequency comb and electro-optical modulator [10]. However, these methods have limited TBWP, which are caused by limited time-width (several ns), small-time aperture (usually several tens of ns), and limited central frequency and bandwidth due to the electric baseband signal and the modulation index. In order to overcome the limited TBWP, optical beating of one optical carrier and another laser with wavelength sweeping is proposed [11], [12]. But the signal quality is deteriorated due to the non-coherent phase relation between two lasers and broadening the dynamic linewidth of the semiconductor laser during wavelength sweeping. Recently, optical injection with a variable injection strength to a semiconductor laser at Period-one (P1) oscillation state has been proposed to generate an LFM signal with a tunable center frequency and large bandwidth [13], [14], which shows a huge potential for the requirements of the modern radar system.

With increasing applications of the modern radar system, single radar signal fails to address the requirement of multiple functionalities and high performance [15]. Compared to a single-band radar, a radar with a dual/multiple-band radar signal (usually with dual/multiple-LFM signal) can provide a higher range resolution, and wider detection range due to the data fusion of two frequency bands [16]. The basic principle involved with a dual-LFM signal generation is the use of single or dual-band LFM baseband signal generated from electrical waveform generator, which is further modulated by a high-order

Manuscript received December 6, 2019; revised March 21, 2020 and April 25, 2020; accepted May 4, 2020. Date of publication May 8, 2020; date of current version October 1, 2020. This work was supported in part by the National Natural Science Foundation of China under Grant 61650110515, Grant 61422108, and Grant 61527820, in part by the National Key R&D Program of China under Grant 2018YFB2201803, and in part by the Fundamental Research Funds for the Central Universities. *(Corresponding authors: Bikash Nakarmi and Shilong Pan.)*

Hao Chen, Limin Zhang, and Snehi Bassi are with the Ministry of Education, Key Laboratory of Radar Imaging and Microwave Photonics, Nanjing University of Aeronautics and Astronautics, Nanjing 210016, China (e-mail: hao_mwp@nuaa.edu.cn; zlmin@nuaa.edu.cn; bassisnehi@nuaa.edu.cn).

Pei Zhou is with the School of Optoelectronic Science and Engineering, Soochow University, Suzhou 215006, China (e-mail: peizhou@suda.edu.cn).

Bikash Nakarmi and Shilong Pan are with the Ministry of Education, Key Laboratory of Radar Imaging and Microwave Photonics, Nanjing University of Aeronautics and Astronautics, Nanjing 210016, China (e-mail: bikash@nuaa.edu.cn; pans@ieee.org).

Color versions of one or more of the figures in this article are available online at https://ieeexplore.ieee.org.

Digital Object Identifier 10.1109/JLT.2020.2993368

electro-optic modulator for optical frequency multiplication, such as dual-parallel Mach-Zehnder modulator (DP-MZM) [17], polarization multiplexing dual-parallel Mach-Zehnder modulator (PM-DPMZM) [18], dual-polarization quadrature phase-shift keying (DP-QPSK) modulator [19], dual-polarization Mach-Zehnder modulator (DPol-MZM) [20], and cascaded MZMs [21]. These techniques, however, provide flexibility in choosing different carrier frequencies but are challenging to tune them separately, complex in structure, and costly. Additionally, the limited modulation index and the bandwidth of the baseband LFM signal restricts the center frequency and the bandwidth of the generated dual-LFM signal.

In this paper, we propose a simple photonics approach to generate an identical or complementary chirp dual-band LFM signal by injecting two optical beams to a distributed-feedback (DFB) laser in P1 oscillation state. Also, it is noteworthy that we use only a sinlge injection-strength controller (composed of a modulator and an arbitary wavelength generator) for the generation of dual-LFM signal whether it is of identical chirp or of complementary chirp. Among two injected beams, the power of the first beam is controlled by an injection-strength controller, whereas the injection parameters of the second beam are constant. With a varying power of the first beam through injection-strength controller, the emission frequency of the DFB laser shifts. Hence, by controlling the power of the first beam, two LFM signals are generated by optical-to-electrical conversion of the output spectrum of the DFB laser. We further analyze the redshift of the emission frequency of the DFB laser with different frequency detunings. Based on the analysis and the demonstration results, the proposed scheme has capability of not only generating a dual-LFM signal with identical chirp but also generating a dual-LFM signal with complementary chirp. Also, the center frequency and the bandwidth of generated LFM signals can be tuned independently by changing the frequency and power of the injected beams. In the proof-of-concept experiment, dual-LFM signal with identical chirp (20–25 GHz and 26.5–31.5 GHz) and complementary chirp (up-chirp: 25–32 GHz, and down-chirp: 16–23 GHz) in the same temporal period of 1.3 μs has been obtained, respectively. The TBWP of the generated dual-LFM signal is about 9100. Additionally, frequency tunability and autocorrelation function of the generated dual-LFM signal is also investigated.

II. Principle and Experiment Setup

Semiconductor laser exhibits various nonlinear dynamics on injecting an optical beam with different injection ratio and frequency detuning. In this paper, we mainly focus on the analysis of P1 oscillation state and redshift of the emission frequency of the semiconductor laser, which are used for generating a tunable and reconfigurable dual-LFM signal. P1 oscillation is a typical nonlinear dynamics of optical injection to a semiconductor laser [22]. The injected beam from the master laser (ML) and the emission mode of slave laser (SL) are dynamic competitive up to resonance in the laser cavity of SL. The output of the SL after an optical injection in the time domain is a cyclic curve with one period, where the period is equal to the reciprocal of the frequency detuning between the injected beam and the shifted mode of SL. Hence, P1 oscillation state is suitable for stable microwave signal generation with large tunability. For semiconductor lasers, the emission frequency of the free-running semiconductor laser can be expressed as [23].

$$f_m = \frac{1}{2\mu L} m \tag{1}$$

Where f_m is the emission frequency of the m^th longitudinal mode of the semiconductor laser, *m* is the number of longitudinal mode, μ is the refractive index of the active layer in the semiconductor laser, which depends on the number of the charge carrier, *N*, in the laser cavity, and *L* is the cavity length. With an optical injection, the charge carrier density and the refractive index in the cavity of SL changes and hence, the emission frequency changes. The shift in emission frequency is known as redshift in the semiconductor laser.

Compared with a single beam injection, dual-beam injection system has more complex dynamics. The SL under dual-beam injection can be described by the rate equations as [24]:

$$\begin{aligned}\frac{dA}{dt} &= \left[-\frac{\gamma_c}{2} + i\left(\omega_0 - \omega_c\right)\right] \\ &\quad \times A + \frac{\Gamma}{2}\left(1 - i\alpha\right) gA + \eta\left(A_1 e^{-i\Omega_1 t} + A_2 e^{-i\Omega_2 t}\right) \\ \frac{dN}{dt} &= \frac{J}{ed} - \gamma_s N - g\frac{2\varepsilon_0 \mu^2}{\hbar\omega_0}|A|^2 \end{aligned} \tag{2}$$

Where *A* is the complex field amplitude at the free-running angular frequency ω_0 of SL, γ_c is the cavity decay rate, and ω_c is the resonance frequency of the slave laser cavity. Γ is the confinement factor, which gives the spatial overlap between the active gain volume and the optical mode volume, α is the linewidth enhancement factor, *g* is the optical gain, and η is the injection coupling parameter. Here, $A_j = |A_j|^{\mathrm{ei}\varphi\mathrm{j(t)}}$ $(j = 1{,}2)$ are the complex amplitudes of the injection field where φ_j(t) is the phase of the injection field. Ω_j is the offset angular frequency of the injection fields compared to the angular frequency of a free-running SL. *J* is the injection current density, *e* is the electric charge, *d* is the active layer thickness, γ_s is the spontaneous carrier relaxation rate, ε_0 is the free-space permittivity, and $\hbar$ is the reduced Planck's constant.

Figure 1 illustrates the basic principle of the proposed dual-LFM signal generation, which is based on the nonlinear dynamics and the redshift of the emission frequency of DFB laser subjected to an optical injection in P1 oscillation state. Fig. 1(a) shows the simplified block diagram of the proposed scheme where two optical beams from MLs with different frequencies, f_inj1 and f_inj2, are simultaneously injected to SL, a DFB laser, with a free-running frequency, f_s0. The output of the DFB laser is passed through a photoelectric detector (PD) for optical beating to generate the electrical signal. Fig. 1(b) illustrates the injection of two beams to SL for microwave signals generation. In Fig. 1(b-i), two injected beams, f_inj1 and f_inj2, are simultaneously injected to the SL with positive frequency detuning, and optical power, P_1, and P_2, respectively. In Fig. 1(b-ii), the beam, f_inj1, is injected to SL with positive

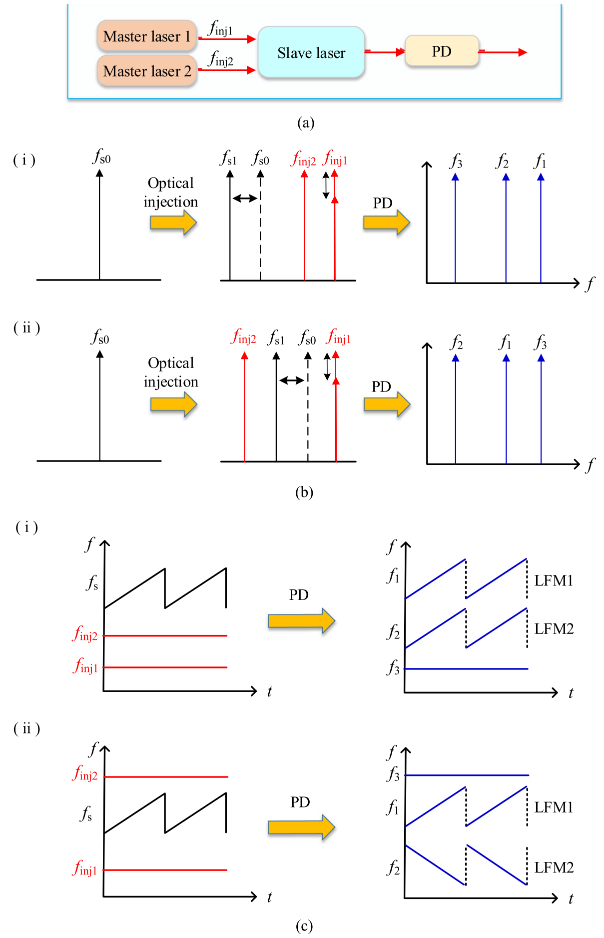

Fig. 1. Basic principle of dual-beam injection to a DFB laser (a) block diagram (b) microwave signal generation with (i) both positive and (ii) opposite frequency detuning, and (c) dual-LFM signal generation with (i) both positive and (ii) opposite frequency detuning.

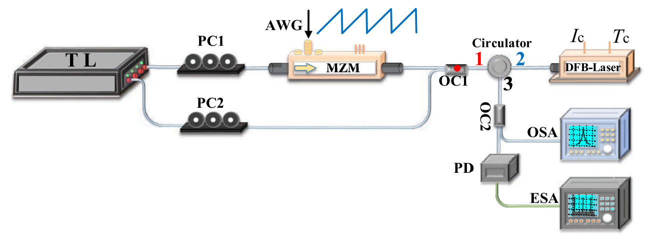

Fig. 2. Experimental setup of dual-LFM signal generation. (TL: tunable laser; PC: polarization controller; MZM: electro-optic Mach-Zehnder modulator; AWG: arbitrary waveform generator; OC: optical coupler; DFB-Laser: distributed feedback laser; PD: photoelectric detector; OSA: optical spectrum analyzer; ESA: electrical spectrum analyzer).

frequency detuning, and the beam, $f_{\rm inj2}$, is injected with negative frequency detuning. Three microwave signals, f_1, f_2, and f_3, are generated by the optical beating of injected beams and the redshifted mode of SL which is equivalent to frequency detuning of $f_{\rm inj1}$-$f_{\rm s1}$, $f_{\rm inj2}$-$f_{\rm s1}$, and $f_{\rm inj1}$-$f_{\rm inj2}$, respectively. It is worth noting that the emission frequency of SL is changed from $f_{\rm s0}$ to $f_{\rm s1}$ with the injection of the optical beams which can be further changed by varying the power of the injection beam. Therefore, the generated microwave signals, f_1 and f_2, can be changed by controlling the injection strength of injected beams either $f_{\rm inj1}$ or $f_{\rm inj2}$, whereas the frequency f_3 remains constant. Hence, by properly controlling the power and the frequency of $f_{\rm inj1}$ and $f_{\rm inj2}$, a dual-LFM waveform can be generated, as shown in Fig. 1(c). The emission frequency, $f_{\rm s}$, can be varied from $f_{\rm s0}$ to $f_{\rm s1}$, in a periodic saw tooth wave fashion in the time domain by varying the power of the injected beam, $f_{\rm inj1}$, where the frequency of $f_{\rm inj1}$ and $f_{\rm inj2}$ are constant. Hence, a dual-LFM signal, which contains LFM1 and LFM2, with the same periodic sawtooth wave can be generated in the temporal-frequency domain. By changing the sawtooth wave to another waveform, the waveform generated by the proposed system can be changed.

LFM1 is generated by optical beating $f_{\rm inj1}$, and $f_{\rm s}$, and LFM2 is generated by optical beating $f_{\rm inj2}$ and $f_{\rm s}$ as illustrated in Fig. 1(c). Since, both beams are injected to SL with positive frequency detuning, the generated dual-LFM signal with identical chirp is generated which is shown in Fig. 1(c-i). On contrary, when two beams are injected to both sides of the emission frequency of SL, complementary chirp dual-LFM signal, one with increasing frequency and another with decreasing frequency, is observed as shown in Fig. 1(c-ii). Besides the dual-LFM signal, microwave signal with constant frequency, f_3, is also generated by optical beating two injected beams, $f_{\rm inj1}$ and $f_{\rm inj2}$, in both cases and does not have any influence on generated LFM signals. The bandwidth of the generated two LFM signals is always the same because it is equal to the total redshift range of $f_{\rm s}$ and can be varied by changing the injection parameters.

Figure 2 shows the experimental setup of the proposed scheme of reconfigurable identical and complementary-chirp dual-LFM signal generation based on dual-beam injection to a semiconductor laser. In the experimental setup, multi-channel tunable laser (TL, Agilent N7714A) is used as two independent MLs that have wavelength tunability from 1527.60 to 1565.50 nm and optical power tunability from 5 to 16 dBm. The DFB laser, Actech LD15DM, is used as an SL whose temperature ($T_{\rm c}$) and current ($I_{\rm c}$) are controlled by a laser diode current and temperature controller, THORLABS, ITC4001. Two optical beams generated from MLs are simultaneously injected to the SL through an optical coupler (OC1) and an optical circulator. Among two injected beams, one optical beam is passed through a polarization controller (PC1) and a Mach-Zehnder modulator (MZM, 10 Gb/s, Lucent 2623NA), which is driven by arbitrary waveform generator (AWG, 120 MHz, Agilent 85110A). The injection strength of the beam is controlled by a near-saw tooth profile control signal, which is generated by the AWG and applied to the MZM. Another beam is injected to SL through a coupler, OC1, and is maintained with constant power. The output of SL is further passed through a PD with a 3 dB bandwidth of 30 GHz for optical-to-electrical conversion to generate the electrical signal, which is monitored by an electrical spectrum analyzer (ESA, 50 GHz, R&S FSU50) and a real-time oscilloscope (Keysight, 32 GHz, DSO-X 92504A), whereas the optical spectrum before PD is measured by an optical spectrum analyzer (OSA, Yokogawa AQ6370C) with a resolution of 0.02 nm.

III. Experimental Results

A. Nonlinear Dynamics of a Semiconductor Laser Under Dual-Beam Injection

Compared to single-beam injection, dual-beam injection to a semiconductor laser presents more complicated nonlinear dynamics, especially in periodic oscillations. Normally, dual-beam injection to a semiconductor laser exhibits three nonlinear dynamics scenarios [24]: (i) Scenario A, where dual-beam injection suppresses the nonlinear dynamics caused by the separately injected beam (dynamics 1 caused by f_{inj1} and f_{s}, and dynamics 2 caused by f_{inj2} and f_{s}). The dynamics of dual-beam injection are not the same as dynamics 1 and dynamics 2. With the same injection parameters, the frequency of microwave signals (f_1 and f_2) generated by dual-beam injection is not the same as that of microwave signal generation under single beam injection. (ii) Scenario B, where the dynamics of dual-beam injection is mainly decided by the dynamics caused by one of the injected beams under single beam injection, such as dynamics 1, meanwhile dynamics 2 has little influence on dynamics 1. With the same injection parameters, the frequency of microwave signal, f_1, generated by dual-beam injection is the same as that of single beam injection, but microwave signal f_2 changes because f_2 is generated by optical beating f_{inj2} and shifted f_{s}. It is because the power of the injected beam f_{inj2} has a weak influence on the dynamics caused by f_{inj1} and f_{s}. (iii) Scenario C, where dual-beam injection does not suppress the dynamics 1 and 2. In this scenario, the power of the injected beams f_{inj1} and f_{inj2} are too weak to shift f_{s0}, so it's difficult to generate an LFM signal.

At first, we verify dual-beam injection to a DFB laser for microwave signals generation, as shown in Fig. 3. Fig. 3(a) shows microwave signals generation by injecting two beams (f_{inj1} and f_{inj2}) with similar power to a DFB laser with opposite frequency detunings (one with positive and another with negative frequency detuning). The black line in Fig. 3(a-i) is the optical spectrum of the free-running DFB laser with an emission frequency of f_{s0}, under a biasing current of 30 mA and controlling temperature of 22.45 °C. Two optical beams, f_{inj1} and f_{inj2}, are separately injected into the DFB laser. On optical injection, the laser cavity forms a stable P1 oscillation state. The blue and red lines in Fig. 3(a-i) represents the output optical spectrum of DFB laser after optical injection by f_{inj1} and f_{inj2}, respectively. We can see that the emission frequency f_{s0} of the DFB laser shifts to f_{s1} and f_{s2}, respectively. Hence, the microwave signals with the frequency equivalent to the frequency difference between f_{inj1} and f_{s1} ($f_1 = f_{\mathrm{inj1}}$-$f_{\mathrm{s1}} =$ 23.22 GHz), and f_{inj2} and f_{s2} ($f_2 = f_{\mathrm{s2}}$-$f_{\mathrm{inj2}} =$ 21.53 GHz) are generated after optical-to-electrical conversion in PD as shown in Fig. 3(a-ii). Further, we simultaneously inject f_{inj1} and f_{inj2} to the DFB laser, where the injection parameters of f_{inj1}, f_{inj2}, and f_{s} are same as that in Fig. 3(a-i), as shown in Fig. 3(a-iii). Due to the nonlinear dynamics in dual-beam optical injection, the emission frequency of the DFB laser shifts from f_{s0} to f_{s3}. Hence, the generated microwave signals, $f_1 = f_{\mathrm{inj1}}$-$f_{\mathrm{s3}} =$ 21.64 GHz, and $f_2 = f_{\mathrm{s3}}$-$f_{\mathrm{inj2}} =$ 18.57 GHz are shown in Fig. 3(a-iv)

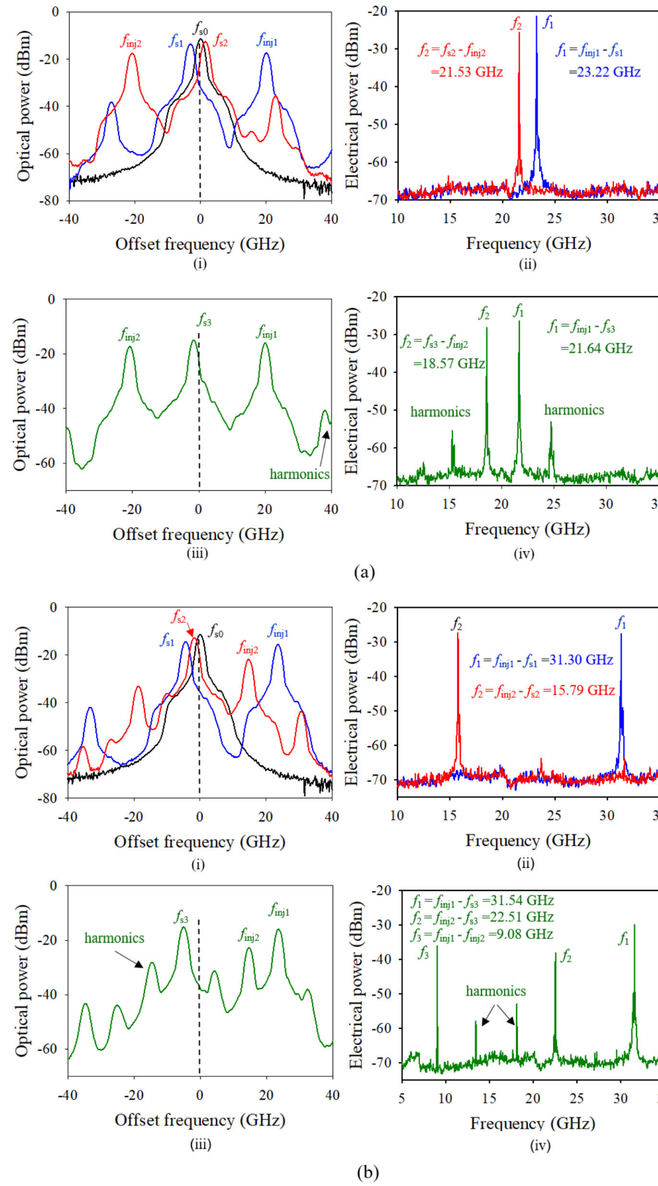

Fig. 3. Experimental result of dual-beam injection to a DFB laser for microwave signal generation with (a) opposite and (b) both positive frequency detuning. (i) frequency shift with a single beam, (ii) electrical signal of single beam injection, (iii) frequency shift with dual-beam injection, and (iv) electrical signal of dual-beam injection.

whereas $f_3 = f_{\mathrm{inj1}}$-$f_{\mathrm{inj2}} =$ 40.21 GHz is not shown due to the limited bandwidth of the PD. From Fig. 3(a), we observe that with dual-beam injection, the generated microwave signals, f_1 and f_2, shift 1.58 GHz and 2.96 GHz, respectively compared to that of single-beam injection. It is due to the fact that the dynamics of dual-beam injection are different from any of the dynamics caused by single beam injection as shown in Fig. 3(a) and referred to as Scenario A. In this case, the microwave signals (f_1, f_2) generated by dual-beam injection are different from those generated by single beam injection. Also, the change in the injection parameter, whether it is injected power or the wavelength detuning of either of the injected beams, f_{inj1} or f_{inj2}, affects the generated microwave signals, f_1 and f_2, lacking the independent tunability.

Next, we inject two beams, both with positive frequency detunings, to the DFB laser for microwave signals generation, where the power of f_{inj2} is about 5 dB less than f_{inj1}. The experiment results are shown in Fig. 3(b). Similar to Fig. 3(a), Fig. 3(b-i) and (b-ii) show the optical spectrum of single beam injection to the DFB laser and the corresponding electrical microwave signal. The generated microwave signals are $f_1 = f_{\text{inj1}}$-$f_{\text{s1}} = 31.30$ GHz and $f_2 = f_{\text{inj2}}$-$f_{\text{s2}} = 15.79$ GHz. Fig. 3(b-iii) shows the optical spectrum when two beams are simultaneously injected into the DFB laser, where the parameters of f_{inj1}, f_{inj2}, and f_{s} are the same as that in Fig. 3(b-i). The emission frequency of the DFB laser shifts to f_{s3} due to the nonlinear dynamics with dual-beam optical injection. Hence, the generated microwave signals are $f_1 = f_{\text{inj1}}$-$f_{\text{s3}} = 31.54$ GHz, $f_2 = f_{\text{inj2}}$-$f_{\text{s3}} = 22.51$ GHz, and $f_3 = f_{\text{inj1}}$-$f_{\text{inj2}} = 9.08$ GHz, as shown in Fig. 3(b-iv). Besides these, we can see multiple peaks. These multiple peaks are the harmonics signals that are generated due to four-wave mixing. These unwanted harmonics have much less power and can be filtered out, and hence have no influence on the generated microwave signals. From Fig. 3(b-ii) and 3(b-iv), we observe that the generated signals, f_1 and f_2, with dual-beam injection shift 0.24 GHz and 6.72 GHz, respectively compared to that of single-beam injection. In this case, dual-beam injection does not suppress the dynamics caused by single-beam injection of the first beam f_{inj1}, but that of the second injection beam f_{inj2} is restrained which is equivalent to Scenario B. Since, beam f_{inj2} has a weak influence on the periodic oscillation caused by beam f_{inj1} and the emission frequency of DFB laser, independent tuning of frequency can be obtained.

On the contrary, dual-beam injection with both negative frequency detunings to DFB laser is not suitable for microwave signal generation due to the small range of redshift of mode in SL, driving the SL into injection locking or mode hopping state. Hence, the LFM signal generation is difficult before the suppression of the emission frequency of the semiconductor laser occurs [22].

B. Analysis of Redshift of the DFB Laser Subject to Dual-Beam Injection With Variable Injection Strength of f_{inj1} in Scenario B

Based on the analysis in part A, we verify that the generation of multi-microwave signals with dual-beam injection to a DFB laser, and Scenario B is suitable for generating microwave signals with independent tuning feature. In this section, we analyze frequency variation of the generated microwave signals by changing the power of the main injected beam, f_{inj1}, keeping the power of another beam, f_{inj2}, constant at 5.5 dBm. The effect of changing the injection strength of f_{inj1} is illustrated in Fig. 4 for both cases: dual-beam injection with opposite frequency detunings and positive frequency detunings. Fig. 4(a-i) shows the output spectrum of the DFB laser for different injection power of f_{inj1} when two beams are injected with opposite frequency detunings. The power of f_{inj1} is increased from 5.5 dBm to 13.5 dBm with an interval of 1 dBm. We observe that the frequency of MLs, f_{inj1}, and f_{inj2}, are constant whereas the emission frequency of the DFB laser is shifted to a lower frequency. Figure 4(a-ii) shows the generation of dual-microwave signal with complementary frequency variations on increasing the power of the injected beam f_{inj1}. The generated microwave signals f_1 varies from 20.24 GHz to 24.69 GHz, and f_2 ranges from 15.57 GHz to 20.03 GHz providing the frequency range (bandwidth) of 4.45 GHz and 4.46 GHz, respectively. Besides, a microwave signal with stable frequency, $f_3 = f_{\text{inj2}}$-$f_{\text{inj1}} = 40.1$ GHz, is also generated but is not observed in Fig. 4(a-ii) as it is out of the bandwidth range of the PD.

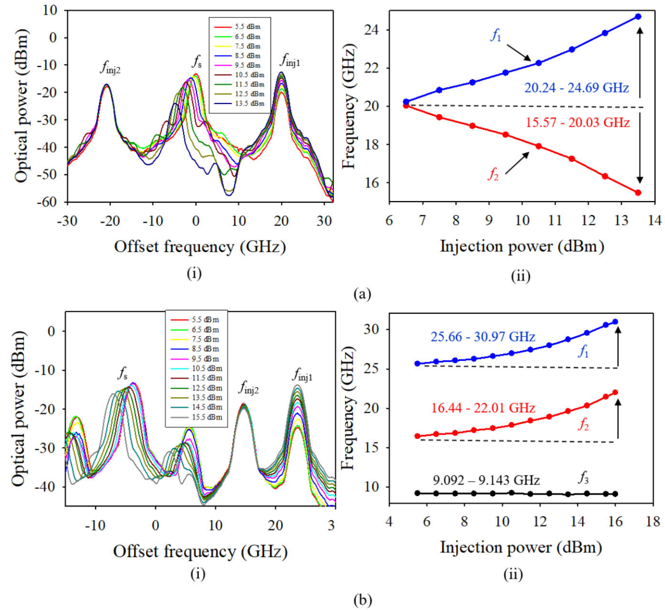

Fig. 4. Optical injection with (a) opposite detuning frequencies and (b) both positive detuning frequencies for tunable microwave signals generation. (i) frequency shift with a change in power of f_{inj1} (ii) electrical output frequency shift.

Next, we inject two beams, both with positive frequency detunings, to the DFB laser. As the power of the injected beam of f_{inj1} increases from 5.5 to 15.5 dBm, the emission frequency of the DFB laser varies similar to that of Fig. 4(a-i), as shown in Fig. 4(b-i). Fig. 4(b-ii) shows the electrical signal outputs, $f_1 = f_{\text{inj1}}$-f_{s}, and $f_2 = f_{\text{s}}$-f_{inj2}, whose frequency increases with approximate-linearly proportional to the power of f_{inj1}, and a constant microwave signal ($f_3 = f_{\text{inj1}}$-f_{inj2}). As the power of injected beam f_{inj1} is changed from 5.5 to 15.5 dBm, f_1 and f_2 are changed from 25.66 to 30.97 GHz and 16.44 to 22.01 GHz with bandwidth of 5.31 GHz and 5.57 GHz, respectively.

The experimental results illustrated in Fig. 4 verifies dual-LFM signal with identical or complementary chirp and approximately linear variation can be obtained by controlling the optical power of the injected beam, f_{inj1}, in Scenario B. The bandwidths of the generated LFM signals are equal to the frequency shift of the mode of SL.

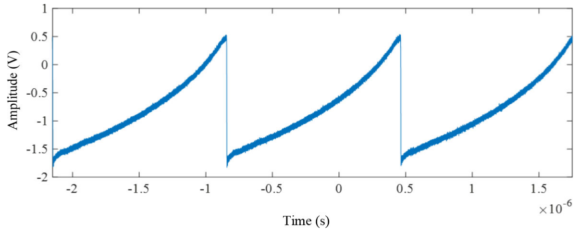

Fig. 5. The electrical control signal S(t) with a near-saw tooth profile for injection-strength controller.

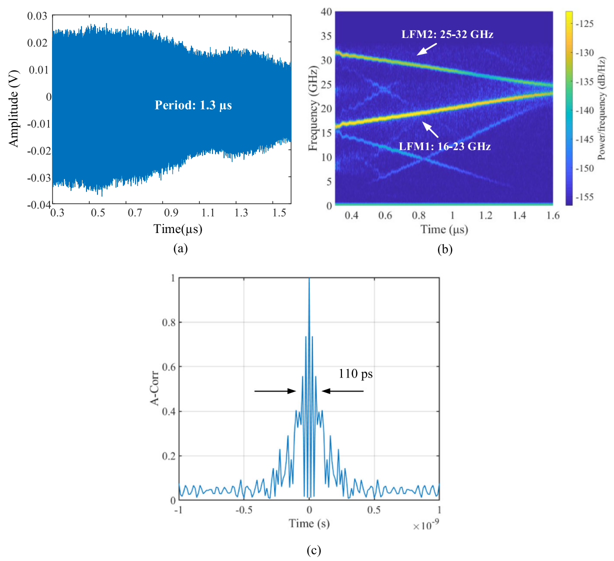

Fig. 6. Dual-LFM signal generation with opposite frequency detuning. (a) temporal waveform, (b) instantaneous frequency-time diagram, and (c) autocorrelation function.

C. Dual-LFM Waveform Generation in Scenario B

In order to generate a dual-LFM waveform, we add an injection-strength controller to modulate the power of the injected beam, f_{inj1}. The injection-strength controller is composed of a 10-Gb/s MZM and an electrical control signal S(t) with a near-saw tooth profile generated by a 120-MHz AWG. Fig. 5 shows the measured electrical control signal S(t) with a period of 1.3 μs and an amplitude of 2.5 V.

Two beams, one with the injection-strength controller, f_{inj1}, and another with constant power, f_{inj2}, are injected to the DFB laser under two cases: (1) two beams with opposite frequency detunings and (2) both beams with positive frequency detunings. The another case, both beams injected with negative frequency detunings, is not considered because of the limited periodic oscillation state and the range of the redshift of the emission frequency of SL before it is suppressed. Fig. 6 shows the experiment result of dual-LFM signal generation by dual-beam injection with opposite frequency detunings. The power modulation of the injected beam f_{inj1} through the injection-strength controller introduces redshift on the emission frequency of SL and hence, dual-LFM signal can be obtained, as shown in Fig. 6. The temporal waveform of the generated dual-LFM signal is measured by a real-time oscilloscope and is shown in Fig. 6(a). The period

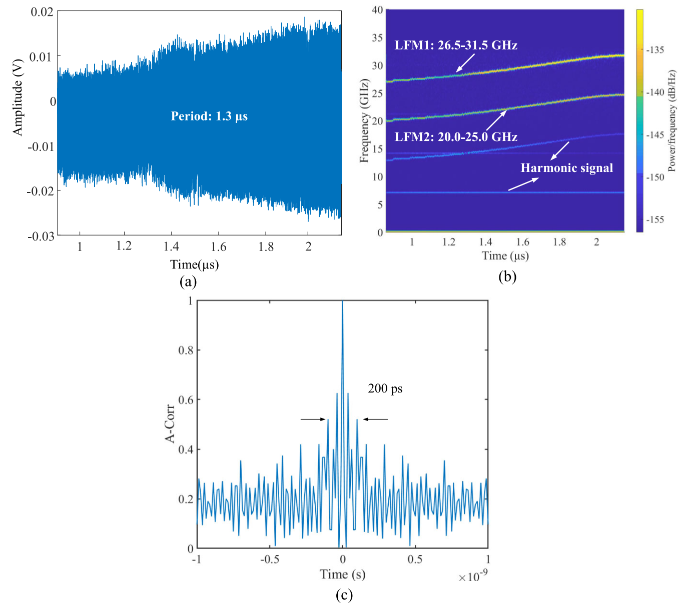

Fig. 7. Dual-LFM signal generation with both positive frequency detunings. (a) temporal waveform, (b) instantaneous frequency-time diagram, and (c) autocorrelation function.

of the generated temporal waveform is 1.3 μs, which matches that of the AWG signal, S(t). Fig. 6(b) shows the instantaneous frequency-time diagram of the generated dual-LFM signals, LFM1 and LFM2, with different center frequencies, 19.5 GHz and 28.5 GHz, respectively and the bandwidth of 7 GHz (LFM1: 16.0 to 23.0 GHz, LFM2: 25.0 to 32.0 GHz). The TBWP of the generated dual-LFM signal is calculated to be 9100. Fig. 6(c) shows the autocorrelation function of the generated LFM signal, which has a full width at half maximum (FWHM) of 110 ps, indicating a pulse compression ratio as high as 11818 [25]. Hence, the theoretical value of the range resolution (r) of the generated dual-LFM signal is $r = c/2B = 2.14$ cm, where c is the velocity of dual-LFM signal in the air, and B is the bandwidth of the generated LFM signal.

Figure 7 shows dual-LFM signal generation by dual-beam injection to the DFB laser with both positive frequency detunings. The temporal waveform and instantaneous frequency-time diagram of the generated dual-LFM signal is shown in Fig. 7(a) and (b), respectively. In this case, two identical LFM signals (LFM1, LFM2) are generated with the same bandwith of 5 GHz (LFM1: 26.5 GHz - 31.5 GHz, LFM2: 20 GHz - 25 GHz) and different central frequencies of 29 GHz and 22.5 GHz, respectively. The TBWP of the generated dual-LFM signal, in this case, is calculated to be 6500. Besides two LFM signals, some harmonics are also observed in Fig. 7(b) which are caused by the optical beating of two injected beams, f_s and optical harmonics generated by four-wave mixing. The unwanted harmonic signals have less power compared to desired LFM signals and are also not intersected with dual-LFM signal. These unwanted harmonics can be filtered out by using optical or electric filters. The autocorrelation function of the generated dual-LFM signals is shown in Fig. 7(c). The FWHM is calculated as 200 ps,

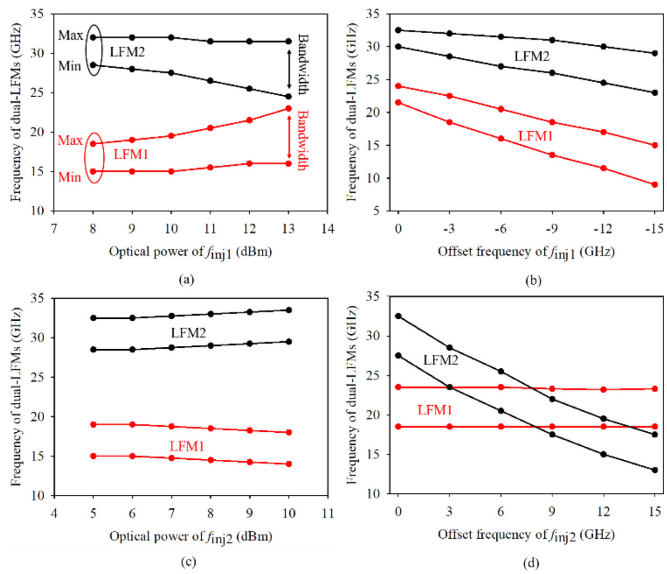

Fig. 8. The tunability analysis of the generated dual-LFM signal with opposite frequency detuning with (a) change in the optical power and (b) change in the frequency of f_{inj1} (c) change in the optical power and (d) change in the frequency of f_{inj2}.

indicating a pulse compression ratio as high as 6500, and the range resolution is about 3.0 cm.

From Fig. 6 and Fig. 7, we can observe that there exist some variation on the amplitude of generated LFM signals. It is because of the decrease in the power of the SL mode on increasing the power of the injected beam. The power of the injected beam can be limited to small range inorder to improve the power flatness of the LFM signal. But, this will also limit the amount of the redshift of f_{s}, as a result, the bandwidth of the generated LFM signal is limited to a small range. Hence, there is a trade-off between the bandwidth and the power flatness of the generated LFM signals. Also, the frequency response of PD and the variation on the attenuation parameters with the frequency of the electrical cables that are used in the experiment deteriorate the power flatness of the generated LFM signals. The power flatness of the generated LFM signal can be improved by using a semiconductor laser with larger redshift cability or adding an optical or electrical amplifier to compensate for the power difference.

D. Tunability Analysis of the Center Frequency and the Bandwidth of the Generated Dual-LFM Signal in Scenario B

In this section, we analyze the tunability of center frequency and bandwidth of the generated dual-LFM signal in Scenario B by varying the injection parameters: power and frequency of the injected beams.

At first, we analyze the effect of changing the injection parameters of f_{inj1} on the tunability of the generated dual-LFM signal. The power and frequency of injected beam f_{inj1} are set as 8 dBm and 193.228 THz, respectively. Then the power f_{inj1} is modulated by the injection-strength controller; meanwhile, the power and frequency of the injected beams, f_{inj2}, is kept constant at 5.5 dBm and 193.181 THz, respectively. In Fig. 8(a), "Max" and "Min" refer to the maximum and minimum frequency of the generated LFM signal, respectively. The frequency difference between "Max" and "Min" is the bandwidth of the LFM signal. With f_{inj1} at 8 dBm and modulated by injection-strength controller, the Max and Min of LFM1 and LFM2 are recorded as (15.0 GHz and 18.5 GHz) and (28.5 GHz and 32.0 GHz), respectively as indicated by circles in Fig. 8(a), providing the bandwidth of 3.5 GHz. On increasing the power of the injected beam, f_{inj1}, from 8 to 13 dBm with an interval of 1 dB, the bandwidth increases from 3.5 GHz (LFM1: 15.0∼18.5 GHz, LFM2: 28.5∼32.0 GHz) to 7 GHz (LFM1: 16.0∼23.0 GHz, LFM2: 25.0∼32.0 GHz), for both LFM signals. Next, the frequency of the injected beam, f_{inj1}, is varied maintaining the power of f_{inj1} at 11 dBm. In this case, the parameters of f_{inj2} are kept same with that in Fig. 8(a). In the experiment, we decrease f_{inj1} from 193.2355 THz with an interval of 3 GHz. We observe that as the frequency of the beam, f_{inj1}, decreases, the bandwidths of both LFM signals increase from 2.5 GHz (LFM1: 22.0∼24.5 GHz, LFM2: 30.0∼32.5 GHz) to 6 GHz (LFM1: 9.5∼15.5 GHz, LFM2: 23.0∼29.0 GHz), as shown in Fig. 8(b). From Fig. 8(a) and (b), we can see that in Scenario B, the injection parameters of beam f_{inj1} influences the bandwidth and center frequency of generated LFM signals simultaneously. It is because the dynamics of f_{inj1} and f_{s} is the main dynamics in dual-beam injection, hence, the power or frequency variation of f_{inj1} affects the redshift range of f_{s}.

Similarly, we analyze the influence of f_{inj2} on the tunability of the generated dual-LFM signal by changing the injection parameters of f_{inj2}. First, we vary the power of the injected beam, f_{inj2}, from 5 to 10 dBm with an interval of 1 dB, and the frequency is kept constant at 193.181 THz; the power and frequency of f_{inj1} are kept constant at 11 dBm and 193.2285 THz, respectively. From Fig. 8(c) we can see that with an increase in the power of f_{inj2}, there is no significant change with the bandwidths of two LFM signals and remain constant at 4.5 GHz (LFM1: 15∼19.5 GHz, LFM2: 28.0∼32.5 GHz) but change in the center frequencies of 1 GHz (LFM1: 17 GHz to 16 GHz; LFM2: 30.5 GHz to 31.5 GHz) for both LFM signals. Second, the frequency of the injected beam, f_{inj2}, is increased from 193.232 THz with an interval of 3 GHz maintaining the constant power of injected beam f_{inj2} at 5.5 dBm. In this case, the injected parameters of f_{inj1} are kept same with that in Fig. 8(c). Fig. 8(d) shows change in the frequency of f_{inj2} has no effect on the bandwidth and the center frequencies of the LFM1 because the change in the power of f_{inj2} has less influence on the redshift of f_{s}. Whereas, the center frequencies of LFM2 decreases from 30 to 15 GHz with a constant bandwidth of 5 GHz. The change in the center frequency of LFM2 is inevitable because the frequency of f_{inj2} is changed. It is because that in Scenario B, f_{inj2} is weak to affect the dynamics caused by f_{inj1} and f_{s}. Hence, as the power of f_{inj2} is increased, the bandwidths of the LFM1 and LFM2 are not changed until the power of f_{inj2} is high enough to be in Scenario A. Similarly, as the frequency of f_{inj2} is increased, it has no influence on the dynamics caused by f_{inj1} and f_{s}. Thus, the range of redshift of f_{s}, which is equal to the bandwidth, is stable.

From Fig. 8, we observe that with the change in the injection parameters of f_{inj1}, both the central frequencies and bandwidths of two LFM signals change. In contrast change in the injection parameters of f_{inj2} has little influence on the center frequency and the bandwidth of LFM1 but effects on the center frequency of LFM2. Hence, a dual-LFM signal with independent tunable center frequency and bandwidth can be achieved by controlling the injection parameters of the injected beams. Further, the injected beams with both positive frequency detunings show similar tunability characteristics as that of two beams injected with opposite frequency detunings and hence the results are not illustrated here.

IV. Conclusion

In this paper, we propose and experimentally demonstrate a reconfigurable identical and complementary chirp dual-LFM signal generation using dual-beam injection to a DFB laser. At first, we analyze microwave signals generated with the dual-beam injection to the DFB laser with both positive and opposite frequency detunings, respectively. The semiconductor laser dynamics with dual-beam injection is different from that of single beam injection. Three scenarios are considered with dual-beam injection, among which Scenario B is more preferable for dual-LFM generation and shows the ability to generate an independently tunable dual-LFM signal. By adding an AWG on the main injected beam for controlling injection strength, and another injected beam with constant injection parameters, identical and complementary chirp dual-LFM signals are generated. It is worth noting that the dual-LFM signal generation with negative frequency detunings to both injected beams is difficult to attain because of the limited periodic oscillation state and the limited small range of the redshift of SL. The generated dual-LFM signal has a bandwidth of 7 GHz in the time period of 1.3 μs and the TBWP of 9100. We calculate the autocorrelation function of the dual-LFM signals and the FWHM is found to be 110 ps. The center frequency and the bandwidth of the generated dual-LFM can be varied by changing the power and the frequency of injected beams. We observed that in Scenario B, by changing the power and the frequency of the main injected beam, f_{inj1}, the bandwidth and the center frequency of generated dual-LFM can be varied whereas the change in that of f_{inj2} effects only on the center frequency of LFM2. Therefore, with the proposed scheme, the reconfigurability and the independent tunability in center frequency, bandwidth and different IEEE bands of the generated LFM signals can be achieved. Thus, the proposed scheme of identical and complementary chirp dual-LFM signal generation has enormous potential for the modern radar system.

References

[1] M. I. Skolnik, *Radar Handbook*, 3rd ed. New York, NY, USA: McGraw-Hill, 2008.

[2] H. Kwon and B. Kang, "Linear frequency modulation of voltage controlled oscillator using delay-line feedback," *IEEE Microw. Wireless Compon. Lett.*, vol. 15, no. 6, pp. 431–433, Jun. 2005.

[3] D. Morgan, "*Surface Acoustic Wave Filters: With Applications to Electronic Communications and Signal Processing*." Cambridge, MA, USA: Academic Press, 2010.

[4] D. Gomez-Garcia, C. Leuschen, F. Rodriguez-Morales, J.-B. Yan, and P. Gogineni, "Linear chirp generator based on direct digital synthesis and frequency multiplication for airborne FMCW snow probing radar," in *Proc. IEEE MTT-S Int. Microw. Symp.*, Tampa, FL, USA, Jun. 2014, pp. 1–4.

[5] C. Wang and P. J. Yao, "Photonic generation of chirped microwave pulses using superimposed chirped fiber Bragg gratings," *IEEE Photon. Technol. Lett.*, vol. 20, no. 11, pp. 882–884, Jun. 2008.

[6] C. Wang and P. J. Yao, "Chirped microwave pulse generation based on optical spectral shaping and wavelength-to-time mapping using a Sagnac loop mirror incorporating a chirped fiber Bragg grating," *J. Lightw. Technol.*, vol. 27, no. 16, pp. 3336–3341, Aug. 2009.

[7] M. Li, L. Y. Shao, J. Albert, and J. P. Yao, "Tilted fiber Bragg grating for chirped microwave waveform generation," *IEEE Photon. Technol. Lett.*, vol. 23, no. 5, pp. 314–316, Mar. 2011.

[8] A. Zeitouny, S. Stepanov, O. Levinson, and M. Horowitz, "Optical generation of linearly chirped microwave pulses using fiber Bragg gratings," *IEEE Photon. Technol. Lett.*, vol. 17, no. 3, pp. 660–662, Mar. 2005.

[9] M. Li and J. P. Yao, "Photonic generation of continuously tunable chirped microwave waveforms based on a temporal interferometer incorporating an optically pumped linearly chirped fiber Bragg grating," *IEEE Trans. Microw. Theory Techn.*, vol. 59, no. 12, pp. 3531–3537, Dec. 2011.

[10] A. Kanno and T. Kawanishi, "Broadband frequency-modulated continuous-wave signal generation by optical modulation technique," *J. Lightw. Technol.*, vol. 32, no. 20, pp. 3566–3572, Oct. 2014.

[11] J. M. Wun, C. C. Wei, J. Chen, C. S. Goh, S. Y. Set, and J. W. Shi, "Photonic chirped radio-frequency generator with ultra-fast sweeping rate and ultra-wide sweeping range," *Opt. Express*, vol. 21, no. 9, pp. 11475–11481, 2013.

[12] J. W. Shi, F. M. Kuo, N. W. Chen, S. Y. Set, C. B. Huang, and J. E. Bowers, "Photonic generation and wireless transmission of linearly/nonlinearly continuously tunable chirped millimeter-wave waveforms with high time-bandwidth product at W-band," *IEEE Photon. J.*, vol. 4, no. 1, pp. 215–223, Feb. 2012.

[13] P. Zhou, F. Z. Zhang, Q. S. Guo, and S. L. Pan, "Linearly chirped microwave waveform generation with large time-bandwidth product by optically injected semiconductor laser," *Opt. Express*, vol. 24, no. 15, pp. 18460–18487, Jul. 2016.

[14] P. Zhou, F. Z. Zhang, Q. S. Guo, S. M. Li, and S. L. Pan, "Reconfigurable radar waveform generation based on an optically injected semiconductor laser," *J. Sel. Topics Quantum Electron.*, vol. 23, no. 6, Nov. 2017, Art. no. 1801109.

[15] P. Van Dorp, R. Ebeling, and A. G. Huizing, "High resolution radar imaging using coherent multiband processing techniques," in *Proc. IEEE Radar Conf.*, Apr. 2010, pp. 981–986.

[16] J. Tian, J. Sun, G. Wang, Y. Wang, and W. Tan, "Multiband radar signal coherent fusion processing with IAA and apFFT," *IEEE Signal Process. Lett.*, vol. 20, no. 5, pp. 463–466, May 2013.

[17] D. Zhu and J. P. Yao, "Dual-chirp microwave waveform generation using a dual-parallel Mach–Zehnder modulator," *IEEE Photon. Technol. Lett.*, vol. 27, no. 13, pp. 1410–1413, Jul. 2015.

[18] Q. Guo, F. Z. Zhang, P. Zhou, and S. L. Pan, "Dual-band LFM signal generation by optical frequency quadrupling and polarization multiplexing," *IEEE Photon. Technol. Lett.*, vol. 29, no. 16, pp. 1320–1323, Aug. 2017.

[19] K. Zhang *et al.*, "Photonic approach to dual-band dual-chirp microwave waveform generation with multiplying central frequency and bandwidth," *Opt. Commun.*, vol. 437, pp. 17–26, 2019.

[20] S. Zhu, M. Li, N. H. Zhu, and W. Li, "Transmission of dual-chirp microwave waveform over fiber with compensation of dispersion-induced power fading," *Opt. Lett.*, vol. 43, pp. 2466–2469, 2018.

[21] Y. X. Xu, T. Ji n, H. Chi, S. L. Zheng, X. F. Ji n, and X. M. Zhang, "Photonic generation of dual- chirp waveforms with improved time-bandwidth product," *IEEE Photon. Technol. Lett.* vol. 29, no. 15, pp. 1253–1256, Aug. 2017.

[22] S. C. Chan, S. K. Hwang, and J. M. Liu, "Period-one oscillation for photonic microwave transmission using an optically injected semiconductor laser," *Opt. Express*, vol. 15, no. 22, pp. 14921–14935, 2007.

[23] A. Murakami, K. Kawashima, and K. Atsuki, "Cavity resonance shift and bandwidth enhancement in semiconductor lasers with strong light injection," *IEEE J. Quantum Electron.*, vol. 39, no. 10, pp. 1196–1204, Oct. 2003.

[24] X. Q. Qi and J. M. Liu, "Dynamics scenarios of dual-beam optically injected semiconductor lasers," *IEEE J. Quantum Electron.*, vol. 47, no. 6, pp. 762–769, Jun. 2011.

[25] M. I. Skolnik, *Radar Handbook*, 3rd ed. New York, NY, USA: McGraw-Hill, 2008.

Hao Chen received the B.S. degree in photoelectron system from Huaqiao University, Xiamen, China in 2012 and the ME degree in electronics engineering from Xiamen University, Xiamen, China, in 2016. Currently he is a Ph.D. student in electronics engineering with the Nanjing University of Aeronautics and Astronautics, (NUAA), Nanjing, China. His current research focuses on the areas of semiconductor laser diodes applications for optical generation and processing of microwave signals.

Pei Zhou received the B.S. and Ph.D. degrees from the Nanjing University of Aeronautics and Astronautics (NUAA), Nanjing, China, in 2013 and 2019, respectively. He is currently with the School of Optoelectronic Science and Engineering, Soochow University, as an Assistant Professor. He conducted research at the University of California, Los Angeles, from 2017 to 2018 under a joint-training Ph.D. program. His current research interests include microwave photonics, nonlinear laser dynamics and optical chaos.

Limin Zhang is a Postgraduate of Key Laboratory of Radar Imaging and Microwave photonics with the University of Aeronautics and Astronautics. She received the BS and MS degrees from the Chongqing University of Posts and Telecommunications in 2014 and 2018. Her current research interests include optical injection, SMFP-LD, and microwave photonics.

Snehi Bassi received the B.Eng. degree in electronics and communication engineering from Kathmandu Engineering College, Nepal, in 2016. She is currently working toward the Masters' degree in electronics and information engineering program with the Nanjing University of Aeronautics and Astronautics (NUAA) . Her research interest includes Microwave Photonics, Fabry Pérot Laser Diodes, Digital Signal Processing, and Optical Communication.

Bikash Nakarmi (Member, IEEE) received the B.E. degree in electronics and communication from Tribhuvan University, Kirtipur, Nepal, in 2004, M.E. degree from Harbin Engineering University, Harbin, China, and the Ph.D. degree from the Korea Advanced Institute of Science and Technology, Daejeon, South Korea, in 2008 and 2012, respectively, both in information and communication engineering. He joined the College of Electronic and Information Engineering, Nanjing University of Aeronautics and Astronautics, China, in 2016, where he is currently a Professor with the Key Laboratory of Radar Imaging and Microwave Photonics (Nanjing Univ. Aeronaut. Astronaut.), Ministry of Education. His research has focused on the development of optical blocks used in optical communication and networks using Fabry–Pérot laser diode, bio-sensors based on nano-structures, and microwave photonics. Between 2012 to 2013, he worked as a Research and Development Manager at InLC technology korea and as a Post-doctoral Researcher at Nanjing university (2012-2014), China. From 2014 to 2016, he was a Research Professor at KAIST. He has authored and co-authored over 55 research papers, including over 25 peer-reviewed journals, and 30 papers in conference proceedings. Prof. Nakarmi is member of IEEE, OSA, and Life Time Member of Nepal Engineering Association. Prof. Nakarmi had served as a Committee Member in *SPIE Photonics* ASIA, 2012 and a Reviewer of several peer-reviewed journals.

Shilong Pan (Senior Member, IEEE) received the B.S. and Ph.D. degrees in electronics engineering from Tsinghua University, Beijing, China, in 2004 and 2008, respectively. From 2008 to 2010, he was a "Vision 2010" Postdoctoral Research Fellow at the Microwave Photonics Research Laboratory, University of Ottawa, Canada. He joined the College of Electronic and Information Engineering, Nanjing University of Aeronautics and Astronautics, China, in 2010, where he is currently a Full Professor and the Deputy Director of the Key Laboratory of Radar Imaging and Microwave Photonics (Nanjing Univ. Aeronaut. Astronaut.), Ministry of Education. His research has focused on microwave photonics, which includes optical generation and processing of microwave signals, ultrawideband over fiber, photonic microwave measurement, and integrated microwave photonics. Dr. Pan has authored or co-authored over 290 research papers, Including more than 150 papers in peer-reviewed journals and 140 papers in conference proceedings. Dr. Pan is a Senior Member of the IEEE Microwave Theory and Techniques Society, the IEEE Photonics Society, the IEEE Instrumentation and Measurement Society, and a member of the Optical Society of America. He was selected to receive an OSA Outstanding Reviewer Award in 2015. Dr. Pan is currently a Topical Editor for *Chinese Optics Letters*. He was a Chair of numerous international conferences and workshops, including the TPC Chair of IEEE ICOCN 2015, TPC Chair of the high-speed and broadband wireless technologies subcommittee of the IEEE Radio Wireless Symposium in 2013, 2014 and 2016, TPC Chair of the Optical fiber sensors and microwave photonics subcommittee chair of the OptoElectronics and Communication Conference in 2015, a Chair of the microwave photonics for broadband measurement workshop of International Microwave Symposium in 2015, a TPC Chair of the microwave photonics subcommittee of CLEO-PR, OECC, and PGC 2017 (joint conference), and a TPC Co-Chair of IEEE MWP 2017.